

DPP Activates Integrin-Mediated Anchorage-Dependent Signals in undifferentiated mesenchymal cells

Asha Eapen, Amsaveni Ramachandran, Anne George\*

Department of Oral Biology, University of Illinois at Chicago, Chicago, IL 60612, USA

\* To whom correspondence should be addressed. Department of Oral Biology, University of Illinois at Chicago, Chicago, IL 60612, USA

Tel: 1-312-413-0738; Fax: 1-312-996-6044; e-mail: [anneg@uic.edu](mailto:anneg@uic.edu)

KEY WORDS: DPP, Integrins, FAK, Extracellular matrix, Differentiation, Gene expression, Dentin

Running title: DPP activates anchorage-dependent signals

---

**Background:** DPP mediates activation of anchorage-dependent signals.

**Results:** DPP activates focal adhesion complexes and MAPK signaling in undifferentiated mesenchymal cells and primary pulp cells leading to their terminal differentiation into odontoblast-like cells.

**Conclusion:** DPP on the substrate provides a tight association between the structural and signaling elements in undifferentiated mesenchymal cells.

**Significance:** DPP promotes adhesion based odontogenic cell differentiation.

**Abstract:**

DPP, a major noncollagenous protein of the dentin matrix is a highly acidic protein and binds  $\text{Ca}^{2+}$  avidly and thus linked to matrix mineralization. Here, we demonstrate that the RGD domain in DPP can bind to integrins on the cell surface of undifferentiated mesenchymal stem cells and pulp cells. This coupling generates intracellular signals that are channeled along cytoskeletal filaments and activates the non-receptor tyrosine kinase FAK, which plays a key role in signaling at sites of cellular

adhesion. The putative FAK autophosphorylation site Tyr<sup>397</sup> is phosphorylated during focal adhesion assembly induced by DPP on the substrate. We further demonstrate that these intracellular signals propagate through the cytoplasm and activate anchorage-dependent ERK signaling. Activated ERK, translocates to the nucleus and phosphorylates the transcription factor ELK-1 which in turn coordinates the expression of downstream target genes such as DMP1 and DSP. These studies suggest a novel paradigm which demonstrates that extracellular DPP can induce intracellular signaling which can be propagated to the nucleus and thus alter gene activities.

**Introduction**

Dentin sialophosphoprotein (DSPP), a member of the SIBILING family is a noncollagenous protein synthesized by odontoblasts (1-3). Shortly after DSPP is synthesized, it is cleaved into three polypeptides namely, dentin sialoprotein (DSP) (2, 4), dentin glycoprotein (DGP) and dentin phosphoprotein (DPP) (1, 5). The mouse DSPP gene contains five exons and 4 introns with exons 1-4 and part of exon 5 encoding the DSP protein and the remainder

of exon 5 encodes the DPP protein. Mutation in the DSPP gene has been identified to be associated with the genetic disease dentinogenesis imperfecta type II (6-9). DSPP knock out mice displayed dentin defects with less mineralized dentin and wider unmineralized predentin (10). The intact DSPP protein has not yet been isolated from the dentin matrix. Published reports have shown the expression pattern of DSP and DPP as specific markers for terminally differentiated odontoblasts (11, 12).

Dentin phosphophoryn (DPP) also called as “phosphophoryn” is a highly acidic protein and is the major noncollagenous matrix component of dentin (13-15) .

The molecule is so called as it is considered to be a “phosphate carrier” (16). DPP is exceedingly rich in aspartic acid and serine residues(DSS)<sub>n</sub>, and about 90% of the serine residues are phosphorylated(17,18). This enables DPP to have a strong affinity for calcium ion and thus it significantly promotes the growth of hydroxyapatite crystals when bound to collagen fibrils in vitro (19-21). Published reports have implicated that DPP functions as a signaling molecule like some members in the SIBLING family(22). Reports have shown that stimulation of MC3T3-E1 cells by DPP could drive cell differentiation into osteoblast phenotype by activation of the MAPK pathway (23). The use of DPP conditional knockout mice revealed the distinct roles of DSP and DPP in dentin mineralization (11).

DPP contains a conserved RGD domain at the N-terminus implicating a functional role in initiation of integrin-mediated intracellular signaling pathways. The binding of ligands to integrin often trigger intracellular signals that are transmitted through the actin-cytoskeleton by assembly

of specialized structures called focal adhesion kinase (FAK) (24, 25) . FAK a potential signaling molecule, associates with paxillin and can trigger a diverse downstream signaling cascade. Published reports have shown PI3K/Akt pathway, c jun pathway and p53 pathway are some of the downstream signaling pathways that are activated (26, 27). Along with FAK, ELK-1 an ETS domain transcription factor family is thought to play a crucial role in the regulation of signaling cascades that ultimately impacts cell proliferation, differentiation, cell spreading and migration (28).

However, the RGD mediated functions of DPP have not been explored. In this report we investigate the signaling pathway activated by immobilized DPP. We hypothesize that integrin-mediated adhesion of undifferentiated embryonic mesenchymal stem cells such as C3H10T1/2 and primary dental pulp cells bind to immobilized DPP and this results in the formation of a multi-protein scaffolding complex and signaling unit. The formation of this complex might promote the activation of signal transduction pathways like MAP kinase resulting in cell differentiation.

## **Materials and Method**

### **Cell Culture**

Mouse embryonic mesenchymal cells (C3H10T1/2) cells were cultured in BME medium supplemented with 10% FBS and 1% penicillin-streptomycin. Primary dental pulp cells were isolated from day 3 mice and were grown in  $\alpha$ -MEM media supplemented with FBS and penicillin-streptomycin. 12-16 hrs before the start of the experiment, the cells were cultured in BME medium or  $\alpha$ -MEM medium supplemented with 1% FBS. Non-tissue culture grade 6 well plates were coated with recombinant DPP (750ng/ml) in

carbonate buffer. The cells were rinsed with PBS, trypsinized and seeded at 80% confluency. C3H10T1/2 cells seeded on 6 well plates coated with carbonate buffer served as control.

### **DPP Coating on non tissue culture plates**

Non tissue culture plates coated with DPP were prepared by soaking the plate with 750ng/ml of DPP in 20 mM carbonate buffer, pH 9.3, overnight at 4°C in a humidified atmosphere for 2 days. Before use, the protein solution was removed and the plates were rinsed twice in PBS.

### **Cell Culture Transfections**

Transient transfection of ELK plasmid and empty vector (kind gift from Alpin A, Albany medical college, NY) into C3H10T1/2 cells seeded on DPP coated plates was performed using Superfect (Qiagen, CA). After 48 hours of transfection these cells were stained for ELK. Transfection performed on tissue culture plate followed by staining with ELK was used at positive control. Transient transfection was also performed with mRFPruby-actin (kind gift from Müller-Taubenberger A, Ludwig Maximilians University of Munich, Germany) constructs using Fugene HD (Promega, WI).

### **Quantitative Real Time PCR**

RNA was extracted according to the manufacturer's recommended protocol by using Trizol (Invitrogen). RT-qPCR was performed with DNase I (Promega) treated RNA. A total of 1µg of total RNA was reverse transcribed for 90 min at 50°C with Superscript III (GIBCO). After RNA extraction, quantitative real-time PCR (qPCR) analysis was carried out using ABI Step One Plus machine. Expression for OCN, DMP1, DSP, RUNX2, BSP, OPN,

BMP4, MMP9 and GAPDH transcripts were analyzed by qPCR during its linear phase. The relative gene expression level was estimated by using the  $2^{-\Delta\Delta C_T}$  method where  $C_T$  value = log-linear plot of PCR signal versus the cycle number.  $\Delta C_T = C_T$  value of target gene -  $C_T$  value of GAPDH. Primers were obtained from Qiagen. Fig S1 shows the primer sequences.

### **Immunofluorescence**

Cells were cultured on rDPP coated non-tissue culture graded glass cover slips for various time points. Cells were fixed in 4% paraformaldehyde, then permeabilized with 0.1% Triton X-100 in PBS for 5 min and rinsed twice with wash buffer. After blocking for 30 min, the cells were then incubated overnight in primary antibody namely, anti-FAK, anti-Paxillin anti-ELK and anti-phospho ERK1/2 followed by incubation with a Cy3-conjugated secondary antibody for 1 hr. After washing the cells three times with PBS the cover glass was mounted using mounting media (Vector shield, CA) and visualized with an Axio observe D1 Fluorescence Microscope (Zeiss, NY) equipped with Axiovision imaging software (Zeiss, NY). Actin staining (1:100) was done on these cells at different time points followed by DAPI staining for the nucleus.

### **Western blot Analysis**

Activation of the focal adhesion complex and the MAP kinase pathway was determined by western blot analysis. Total proteins were extracted from C3H10T1/2 cells grown on DPP coated plates with or without mineralization media using M-per reagent (Pierce, IL). A total of 35µg of the protein were resolved on a 10% SDS-PAGE gel under reducing conditions. After electrophoresis, the proteins were electro-transferred onto nitrocellulose

membrane (Bio-Rad Laboratories, CA), blocked with 3% BSA in 1X PBS, probed with either anti-FAK, anti-paxillin, anti-Erk1/2, anti-phospho FAK, anti-phospho paxillin, anti-phospho Erk1/2 (1:500) (Santa cruz, CA), anti-DMP1 (1:500) (20) and anti-DSP (1:2000) (20). HRP-conjugated goat anti-rabbit IgG were used for detection (Chemicon International, CA). Lightening chemiluminescence reagent (Perkin-Elmer Life Sciences, MA) was used as substrate for HRP. Each membrane was then carefully washed, treated for 5 min with a stripping buffer to eliminate previous reaction (Pierce, IL), washed with PBS and processed as above with anti-tubulin (1:10,000, Sigma, MO) antibody and HRP conjugated goat anti-mouse IgG.

### **Identification of cell surface receptor**

$1 \times 10^4$  C3H10T1/2 cells were preincubated with each of the antibodies for  $\alpha v$ ,  $\alpha 4$ ,  $\alpha 5$ ,  $\beta 5$ ,  $\beta 4$ ,  $\beta 3$  (1:50, Cell Signaling, MA) or  $\beta 1$  (kind gift from Carbonetto S, McGill University, Montreal, Quebec) for 2 hours on a rotor at 37°C. Following incubation, the cells were seeded on DPP coated plate and incubated for 24 hrs at 37°C. C3H10T1/2 cells seeded on DPP coated plates were used as control. Confocal images (Zeiss, NY) of the cells were taken.

### **Isolation of the cell surface receptor**

C3H10T1/2 cells were treated with rGST-DPP (1mg/ml) for 1 hr at 4°C to ensure binding but not endocytosis. The cells were then washed with ice cold PBS three times after which the membrane proteins were isolated using Pierce reagent. The membrane proteins were then incubated with sepharose beads overnight at 4°C. The beads were then washed with PBS containing 150mM NaCl. The bound proteins were eluted with glutathione, dialyzed against 1mM Tris and

lyophilized. The lyophilized protein was redissolved in 50  $\mu$ l of PBS and immunoblot was performed with integrin alpha v antibody (1:500, cell signaling, MA) and  $\beta 1$  integrin antibody.

### **Transient transfection for $\beta 1$ integrin siRNA**

C3H10T1/2 cells were grown to 60% confluency on DPP coated plates and were transfected with  $\beta 1$  integrin siRNA (0.5  $\mu$ g) or scrambled siRNA duplexes (0.5  $\mu$ g) (Santa cruz, CA) as a control using siRNA transfection reagent (Santa Cruz, CA). Cell attachment was observed and photographed after 24 h.

### **Blocking experiments with RGD peptide**

To confirm the involvement of the RGD domain in mediating cell attachment, confluent  $1 \times 10^4$  C3H10T1/2 cells / mL were incubated for 1hr with 1mM and 2mM RGD peptide (Gly-Arg-Gly-Asp-Asn-Pro) in BME media (GibcoBRL) on a rotor at 37°C in an incubator for 2 hrs prior to plating them on DPP coated plates. The cells were allowed to attach for 24 hours. The adherent cells were fixed, stained with 0.5% toluidine blue, and counted manually. Cells seeded on tissue culture plate were used as control. The experiments were performed in triplicate and standard errors of the cell numbers were determined. Proteins were extracted as per the above protocol and western blots were performed.

### **Preparation of Self-Assembled Monolayers (SAMs)**

Gold substrates were prepared by evaporating Titanium (4 nm) followed by Gold (25 nm) onto glass cover slips using the BOC EDWARDS AUTO 500 System with FL400 chamber (Edwards Ltd., Wilmington, MA). A PDMS stamp

with the selected pattern was coated with a solution of 1mM Hexadecanethiol (HDT) in ethanol. The stamp was then placed on the gold substrate for approximately 30 seconds following which they were separated and the substrate was rinsed with absolute ethanol and dried under a stream of nitrogen. The HDT coated substrate was then immersed overnight in an ethanolic solution of maleimide-terminated disulfides mixed with tri(ethylene glycol)-terminated disulfide (MAL-EG3) in a ratio of 1:99 (final concentration of disulfide was 1 mM) to coat the areas surrounding the HDT islands. A PDMS cylinder (inner diameter 130mm, outer diameter 220mm and height 150mm) was placed on the monolayer substrate. The monolayers were then treated with a 1 mM solution of RGD peptide (in 1X PBS, pH 7.4) for 30 mins followed by immersion in DPP (1 µg/ml in 1X PBS, pH 7.4) solution overnight. The substrates were rinsed with absolute ethanol and dried under a stream of nitrogen between all steps and solution changes. C3H10-T1/2 cells were then seeded on the substrate at a cell density of 500,000 cells/substrate and allowed to attach for 4 hrs in a 37°C incubator with 5% CO<sub>2</sub>. After cell attachment the substrate was rinsed thrice with serum free media to remove the unattached cells and observed under a microscope to check for cell attachment on the pattern. The media was changed to BME containing 0.5% FBS and cells were left overnight in a cell culture incubator. Cells were then fixed and stained with actin and DAPI.

### **Inhibition of ERK1/2**

Cells were cultured as described above and were treated with 30 µM of PD98059 inhibitor (Biomol) – a specific inhibitor for the ERK1/2 MAP kinase pathway. Cell lysates were harvested at 4 and 24 hr time points and western blotting and immunofluorescence were performed as

described above with anti-ERK1/2 antibody and anti-phospho ERK1/2 antibody.

### **Immunoprecipitation**

FAK antibody was mixed with protein-A beads and incubated on a shaker for 2 hours. 50µg total protein from C3H10T1/2 cells grown on DPP coated plates were mixed with the beads and incubated overnight. The beads were then washed three times in 1X PBS to remove non-specific binding. SDS-PAGE loading dye was added to the beads and boiled for 5 minutes. The supernatant was resolved on a 10% SDS gel and immunoblotted with paxillin antibody. Immunoprecipitation performed in the absence of FAK antibody served as control.

### ***In Vitro* Assay to determine differentiation of mesenchymal cells to terminally differentiated odontoblast-like cells**

Mineralization microenvironment was induced by the addition of 10 mM β-glycerophosphate and 100 µg/ml ascorbic acid (Sigma-Aldrich., MO) along with 10 nM dexamethasone (Sigma-Aldrich., MO) in the growth media. Total RNA and total proteins were extracted at 7, 14, and 21 days from C3H10T1/2 cells grown on DPP coated plates.

### **von Kossa Staining for phosphates in the mineralized nodule**

von Kossa staining was performed to determine the presence of phosphate in the mineralized nodules. C3H10T1/2 cells were grown to 60% confluency on DPP coated plates and the growth media was then replaced with mineralization media for 7, 14, and 21 days. The cells were fixed in

formalin for 20 minutes, washed twice with distilled water and then stained with 1% silver nitrate solution (Sigma–Aldrich., MO) for 30 minutes and photographed. Cells grown on DPP coated plates without mineralization media and cells on tissue culture plate with mineralization media were used as controls.

### **Alizarin Red S Staining for Calcium in the mineralized nodule**

C3H10T1/2 cells were grown to 60% confluency on DPP coated plates. The growth media was replaced with mineralization media for 7, 14, and 21 days. The cells were fixed in formalin for 20 minutes at room temperature and washed with distilled water. 2% Alizarin Red solution was added to fixed cells and incubated for 10-20 minutes. The cells were then rinsed with distilled water and were imaged.

## **Result**

### **DPP aids in cell attachment and cytoskeletal organization**

C3H10T1/2 cells were seeded on DPP coated non tissue culture cover glass and cultured for various time points from 30 minutes to 24 hours. The cells were then fixed and stained for actin. Assessment of the attached cells by confocal microscopy (Fig 1) on DPP coated substrate show distinct cell responses such as cell spreading as indicated by their F-actin cytoskeletal structure, formation of multiple filopodia and protrusions of the lamellipodia while cells on DPP non coated plates[(-) DPP] were round and showed no spreading. Cover slip coated with fibronectin served as positive control (Fig 1).

### **Specificity of the RGD domain in cell attachment**

To define the role of RGD domain in cell adhesion, glass slides coated with gold substrate stamped with DPP on one half and GRGDS peptide on the other half with the middle uncoated region were used as substrates for cell attachment assay (Fig 2). Schematic representation of the stamp containing the 2 peptides is shown in Fig 2 A2. C3H10T1/2 cells were seeded on the substrate for 24 hours, fixed and stained with actin. Absence of cell adhesion was seen in the center unstamped section of the substrate (Fig 2 A1). Interestingly, cell adhesion looked robust on both DPP and GRGDS stamped surface.

### **Cell adhesion is abrogated in the presence of RGD blocking peptide**

To confirm the involvement of the RGD domain in mediating cell attachment, C3H10T1/2 cells were incubated with 1mM or 2mM concentrations of GRGDS blocking peptide. Cells were then allowed to attach on a DPP coated cover slip for 24 hrs. The cells were counted and it was observed that 1mM and 2mM concentration of the peptide inhibited cell adhesion when compared to the cells without peptide incubation seeded on DPP coated plate. Results in Fig 2B showed that 2mM concentration of GRGDS peptide had 100% inhibition on cell attachment when compared with that of 1mM concentration.

### **Identification and isolation of the integrin receptors**

The integrin receptor specific for binding of C3H10T1/2 cells to DPP were identified by using a panel of alpha and beta integrin antibodies. When C3H10T1/2 cells were incubated with either  $\alpha$ v,  $\alpha$ 4,  $\alpha$ 5,  $\beta$ 5,  $\beta$ 4,  $\beta$ 3 or  $\beta$ 1 antibodies for 2 hours and then cultured on DPP coated plates for 24 hrs, it was observed that the anti-  $\alpha$ v and  $\beta$ 1

antibodies abrogated cell adhesion (Fig 3A).

Having identified the cell surface receptor as  $\alpha\beta 1$  integrin, we further confirmed by isolating the cell membrane proteins and performing western blot analysis. Results in Fig 3B confirmed the presence of  $\alpha\beta 1$  integrins. Knockdown of  $\beta 1$  integrin in C3H10T1/2 cells performed on DPP coated plate showed a change in morphology within 4 hrs and by 24 hrs were rounded up and seem to be undergoing apoptosis (Fig 3C). Thus,  $\alpha\beta 1$  integrin is necessary for the attachment and survival of C3H10T1/2 cells on DPP substrate.

### **DPP facilitates adhesion-mediated signaling events by organization of focal adhesions**

We next examined the effects of integrin activation on the regulation of FAK and paxillin. We hypothesized that adhesion of C3H10T1/2 cells or primary dental pulp cells to DPP substrate would induce association of focal adhesion kinase (FAK) and paxillin. Immunohistochemical analysis indicated that FAK and paxillin were expressed on the cell membrane of adherent primary dental pulp cells (Fig S2 A, B) and C3H10T1/2 cells at 16(Fig 4 A1) and 24 hours (Fig 4 A2), thereby inducing focal adhesion formation and cell spreading. Z stack analysis performed on images obtained at 24 hour time point shows clear colocalization of FAK with paxillin (Fig 4B). Signaling molecules participating in a pathway are usually in a direct physical association and immunoprecipitation analysis confirmed the *in-vivo* association of FAK and paxillin in C3H10T1/2 cells (Fig 4C). Importantly, we observed the nuclear translocation of FAK on cells adherent to DPP substrate at 16hr and 24hr time points. FAK is a 125-kD protein that is tyrosine phosphorylated and activated in response to integrin clustering. Western blot analysis

(Fig 4D) confirmed FAK activation as Tyr<sup>397</sup> is phosphorylated. This initial phosphorylation is necessary for tyrosine phosphorylation of multiple sites in FAK and in paxillin. Results in Fig 4E show activation of paxillin in C3H10T1/2 cells seeded on DPP coated plates from 30 minutes to 24 hours. Cells plated on carbonate buffer coated slides did not show colocalization of FAK and paxillin at focal adhesions (data not shown).

### **DPP regulates actin assembly**

Actin polymerization drives the extension of sheet-like (lamellipodia) and rod-like protrusions (filopodia) at the cell front. Therefore, to visualize the actin cytoskeleton, C3H10T1/2 cells were transfected with mRFP<sub>rub</sub>-actin plasmid and replated on DPP substrate. Fluorescence images in Fig 5 suggested that ectopically expressed mRFP<sub>rub</sub>-actin was copolymerized with endogenous actin as shown at 8 (Fig 5 A1) and 24 hours (Fig 5 A2). Incorporation of mRFP<sub>rub</sub>-actin was clearly observed in the sub-compartments of the actin cytoskeleton such as microspikes, lamellipodium, filopodium and contractile bundles. Thus, protein assemblies are recruited to the tips of lamellipodia and filopodia that drive the polymerization of actin for protrusion when cells are plated on DPP matrix. It is this actin assembly that generates mechanical signals and transduces them into intracellular signals and favors gene expression.

### **DPP activates the MAP kinase signaling**

MAP kinases are used by cells to transduce signals from the extracellular environment to the nucleus which ultimately results in cell proliferation, differentiation and survival. It has been shown that activation of the extracellular signal-regulated kinase (ERK) could be controlled by adhesion via

integrins (29). To investigate if adherent cells on DPP substrate induced ERK phosphorylation, western blot analysis showed an increase in phosphorylation of ERK1/2 at 4 hr and 24 hr time points (Fig 6A). Interestingly, this activation was suppressed in the presence of the ERK specific inhibitor PD98059. Cells on tissue culture plates were used as control (Fig 6A).

Next we sought to analyze the role of adhesion upon the localization of phospho-ERK. By confocal analysis we determined that in DPP mediated adherent cells, phospho-ERK was localized primarily in the nuclear compartment (Fig 6 B2), and predominantly cytoplasmic in cells plated on tissue culture plates (Fig 6 B1). We then studied the specificity of this activation by using PD98059 a pharmacological inhibitor specific for the ERK1/2 pathway. PD98059 treatment for 24 hrs abrogated the translocation of pERK1/2 into the nucleus (Fig 6 B3). Nuclear localization of pERK1/2 was also observed when primary dental pulp cells were plated on DPP coated plates (Fig S2 C).

### **DPP activates ELK-1 a downstream target of ERK signaling**

Having established that translocation of ERK to the nucleus is regulated by cell adhesion to the DPP substrate, we next analyzed if ELK-1 is a substrate for activated ERK. ELK-1 a transcription factor is a known substrate of ERK and phosphorylation at the C-terminal site is important for its transcriptional activity (30). To this end, we expressed a construct (pCMV5-FLAG-ELK-1) in C3H10T1/2 cells seeded on DPP coated plates as low levels of endogenous ELK-1 is expressed by these cells. Results in Fig 7 show clear nuclear localization of ELK-1 on DPP treated plates. As expected, cells seeded on tissue culture plate did not result in nuclear

translocation of ELK-1 (Fig 7). Interestingly, nuclear localization of ELK-1 was observed when primary dental pulp cells were plated on DPP coated plates (Fig S2 D). Together, these results suggest that activation of ELK-1 is adhesion dependent in response to DPP that correlates with ERK1/2 activation.

### **Blocking RGD inhibits the activation of FAK, Paxillin and ERK1/2**

To confirm that the biological ramifications that we observed, namely activation of FAK, paxillin and ERK1/2 was in response to the RGD domain in DPP, we used a blocking peptide to the RGD domain to study its role in signaling and attachment. As before, we were able to see an activation of FAK, ERK1/2 and paxillin in cells on DPP coated plates. Importantly, this activation was inhibited in the presence of 2 mM concentration of the blocking RGD peptide (Fig 8). Taken together, these data show that RGD in DPP plays a pivotal role in the activation of the adhesion complex which in turn leads to the activation of the MAP kinase signaling pathway leading to cellular differentiation.

### **Attachment of C3H10T1/2 cells on DPP matrix triggers odontogenic differentiation**

Odontogenic differentiation of C3H10T1/2 on DPP coated plates was demonstrated by an increase in the relative expression of markers like DSP, DMP1, Runx2, BMP4, Osteocalcin, OPN, BSP at 4 and 24 hrs after attachment. However, these markers remained unchanged for cells that were seeded on tissue culture plates (positive control) (Fig.9). Most interestingly, we observed an increase in expression of Matrix Metalloprotease 9 at 4 hr when compared with the 24hr time point suggesting a role for MMP9 in DPP mediated cellular

differentiation.

### **DPP stimulates the expression and nuclear translocation of differentiation markers**

Western blot analysis performed on cells grown on DPP coated plates at 4h, 24h and 48h showed up regulation for DSP, DMP1 and DPP (Fig.10A) as compared to the controls obtained from tissue culture plates at 48hrs.

We next explored the subcellular localization of the odontogenic markers, DSP, DMP1 and Runx2 in C3H10T1/2 cells undergoing differentiation. Immunohistochemical staining showed nuclear localization of DSP, DMP1 and RUNX2 (Fig.10B).

### **DPP promotes terminal differentiation of undifferentiated mesenchymal cells**

To detect morphological changes during odontogenic differentiation, C3H10T1/2 cells seeded on DPP coated plates were subjected to mineralization for 7, 14 and 21 days and light microscopic images were obtained. Cells in the presence of mineralization media at 21 day clearly show a change in the morphology of the cells from cobble shaped to spindle shaped (Fig. 11A a) to cellular clustering during mineralization when compared with the control (Fig.11A b). Changes in cellular morphology were also correlated with changes in odontogenic gene expression. mRNA expression for RUNX2, DSP and DMP1 were assessed at time points ranging from 7 to 21 days (Fig. 11B). An initial significant increase in the RUNX2 gene expression was observed at 7 days indicating an early role for RUNX2 in the odontogenic

differentiation program. The mRNA levels of DMP1 were observed to be significantly up regulated at 7 and 14 days and down regulated at 21 days. Interestingly, elevated DSP gene expression was detected at all time points using real time PCR.

Western blots were also performed on total proteins isolated from C3H10T1/2 cells seeded on DPP coated plates grown under mineralization condition for 7, 14 and 21 days. Immunoblots showed significant increase in DSP, DMP1, DPP and pERK1/2 expression from day 7 to day 21 when compared to the control cells which were obtained at 21 days in the absence of differentiation medium (Fig.11C).

### **DPP stimulates mineralized nodule formation in C3H10T1/2 cells**

To provide evidence that DPP supports progression of odontoblast differentiation von Kossa staining was performed at time points 7, 14 and 21 days (Fig. 12A). Odontogenic differentiation and mineralization was observed at all time points on DPP coated plates. At 14 and 21 days of culture, von Kossa staining demonstrated dark deposits in the extracellular matrix demonstrating the presence of phosphate in the calcified nodules. In contrast, cells growth on DPP coated plates in the absence of mineralization for 21 days showed no staining (Fig. 12B). C3H10T1/2 cells grown on tissue culture plate with mineralization media served as control (Fig. 12C).

Odontogenic terminal differentiation of C3H10T1/2 cells was further confirmed by alizarin red staining. C3H10T1/2 cells seeded on DPP coated plates grown in the presence of mineralization medium for 14

and 21 days resulted in staining of the mineralized matrix demonstrating presence of calcium deposits (Fig.13A). Interestingly, no such staining was detected when cells were grown in mineralization conditions on tissue culture plates for 7, 14 and 21 days (Fig. 13B).

## Discussion

Living cells grow and function while being tightly associated with the diverse connective tissue components that form the extracellular matrix (31). The ECM comprises a scaffold on which tissues are organized, provides biological cues and regulates multiple cellular functions. Furthermore, the rigidity of the extracellular environment controls the differentiation of the mesenchymal stem cells (32) and the self-renewal of hematopoietic stem cells (33). The integrins are a large family of cell adhesion receptors, which mediate cell-cell and cell-matrix adhesion (34). Their functions have been implicated in processes like development, immune response, maintenance of tissue integrity, while in pathological conditions they participate in chronic inflammation, invasion of cancer cells and metastasis (35). Major ECM proteins such as fibronectin and collagen bind to several integrins (36, 37). During tooth development, odontoblasts arise from neural crest derived undifferentiated ectomesenchymal cells and undergo sequential steps of differentiation and integrins play an important role in this process (38).

This study describes the cooperative effects between DPP and  $\alpha\beta$ 1 integrin resulting in anchorage of undifferentiated embryonic mesenchymal cells. Knockdown of  $\beta$ 1 integrin confirmed the central role of  $\beta$ 1 integrin in cell attachment. Binding of cell-specific integrins to DPP substrate can have substantial effects on gene expression

by influencing signaling processes. We report that the RGD present at the N terminus of DPP play a specific role in adhesion. Blocking of the RGD binding site present on the cell surface with a peptide resulted in impaired adhesion and differentiation.

The effect of DPP mediated adhesion on activation of FAK, a cytoplasmic protein tyrosine kinase that has been implicated to play an important role in integrin mediated signal transduction was studied. Results from this study show that cells adherent to DPP substrate had increased FAK phosphorylation. This phosphorylation was most pronounced in cells adherent at 4, 8 and 16 hrs. Tyr 397 is a major autophosphorylation site in FAK, which functions as a binding site for Src homology 2 containing proteins in the adhesion complex (39, 40). Interestingly, phospho-FAK was also localized in the nucleus. The role of nuclear FAK in cellular differentiation process is currently unclear, however, a recent study has shown that nuclear FAK targets p53 for degradation and enhances cell survival and differentiation (41). Thus, nuclear localization of FAK in cells attached to DPP substrate might indicate the activation of cell differentiation pathways.

Binding of integrin receptor to DPP substrate should facilitate the recruitment of signaling molecules to the focal adhesion site. Therefore, we examined the focal adhesion complex protein paxillin, as it is a substrate for FAK containing adhesion complex (42, 43). Upon cell adhesion we observed phosphorylation of paxillin. Paxillin is a key scaffolding protein between the focal adhesion complex and the actin cytoskeleton that is known to bind to FAK and mediate FAK recruitment to focal adhesion complexes and that is tyrosine phosphorylated by FAK and or src in

response to integrin engagement (44). Paxillin immunoblots of endogenous FAK precipitates demonstrated *in vivo* association of FAK and paxillin in the complex. The subcellular localization of DPP-mediated FAK-paxillin association showed paxillin being distributed in discrete focal adhesions at the cell periphery, whereas FAK was distributed both in the nucleus and at the cell periphery. In particular, focal adhesion complexes appeared to condense at the leading edges of the cell processes with FAK-paxillin colocalization at these sites.

The integrin-mediated adhesions are multiprotein complexes that link the extracellular matrix to the actin skeleton (31, 45). Cells on DPP substrate show distinct actin organization, with *de-novo* formed actin rich lamellipodium with prominent arrays of parallel filaments containing filamentous actin. Surface membrane receptors such as integrins which mediate cell adhesion to extracellular matrix are known to have a central role in mechanotransduction and can generate mechanical signals which are known to propagate through the cytoplasm much quicker than diffusion-based chemical signals (46).

Published reports suggest that adhesion receptors and their cytosolic partners can regulate trafficking of signaling proteins between the cytoplasm and nucleus which result in the control of transcription (47). Recently it has been shown that activation of MAP kinases can be controlled via integrins (48). Upon integrin-mediated adhesion to DPP, ERK translocates from the cytoplasm to the nucleus. Interestingly this nuclear localization was abrogated in the presence of PD98059 an inhibitor specific for phosphorylated form of ERK1/2. However, blocking of the peptide also inhibited focal adhesion complex and ERK1/2 signaling pathway. In control cells ERK was localized

in the cytoplasm. Published reports demonstrate that ERK accumulation in the nucleus occurs more efficiently in adherent cells, whereas nuclear accumulation of phosphorylated p38 and phosphorylated JNK are unaffected by changes in adhesion (49). In the nucleus, activated ERK efficiently phosphorylates ELK-1 and this is adhesion-dependent. Phosphorylated ELK-1 plays a pivotal role in immediate early gene induction by external stimuli (30). Our findings highlight the importance of cellular adhesion to DPP substrate and activation of ERK, which translocates to the nucleus and transactivates the transcription factor ELK-1.

Cell anchorage to DPP substrate can have substantial effects on gene expression. Undifferentiated mesenchymal cells anchored on DPP substrate had the ability to express transcription and growth factors like BMP4, Runx2, and odontogenic secretory stage-specific phenotypic markers like DMP1 and DSP. Increase in the expression levels of these genes within 24 hrs suggests that cells attached to DPP matrix can activate transcriptional regulation and thereby aid in the differentiation process. Terminal differentiation of undifferentiated mesenchymal cells to functional odontoblast-like cells was confirmed by von Kossa and alizarin red staining of the ECM matrix.

Taken together, these findings suggest that DPP plays a major role in anchorage-dependent signaling events. These events include physical coupling of integrins with extracellular DPP which initiates a mechanical stimulus resulting in the activation of FAK and Paxillin and their interactions at the adhesion complex (Fig 14). The ability of FAK to be present in focal adhesions as well as in the nucleus may be important for its role in regulating anchorage-dependent ERK activation.

Once activated, the signals propagate through the cytoplasm leading to accumulation of activated ERK in the nucleus where it phosphorylates transcription factors like ELK-1 leading to downstream odontogenic gene expression and differentiation of embryonic mesenchymal cells to odontoblast-like cells.

Hallmark of terminal differentiation is the induction of mineralized matrix formation which has been confirmed by von-Kossa and Alizarin Red staining in this study. Thus, extracellular DPP can provide a tight association between the structural and signaling elements in undifferentiated mesenchymal cells.

## References:

1. Feng, J. Q., Luan, X., Wallace, J., Jing, D., Ohshima, T., Kulkarni, A. B., D'Souza, R. N., Kozak, C. A., and MacDougall, M. (1998) *J. Biol. Chem.* **273**(16), 9457-9464
2. Yamakoshi, Y., Lu, Y., Hu, J. C., Kim, J. W., Iwata, T., Kobayashi, K., Nagano, T., Yamakoshi, F., Hu, Y., Fukae, M., and Simmer, J. P. (2008) *J. Biol. Chem.* **283**(21), 14835-14844
3. George, A., Srinivasan, R. S. R., Liu, K., and Veis, A. (1999) *Connect. Tiss. Res.* **40**(1), 49-57
4. Yamakoshi, Y., Hu, J. C., Iwata, T., Kobayashi, K., Fukae, M., and Simmer, J. P. (2006) *J. Biol. Chem.* **281**(50), 38235-38243
5. Yamakoshi, Y., Hu, J. C., Fukae, M., Zhang, H., and Simmer, J. P. (2005) *J. Biol. Chem.* **280**(17), 17472-17479
6. Hart, P. S., and Hart, T. C. (2007) *Cells, tissues, organs* **186**(1), 70-77
7. MacDougall, M., Dong, J., and Acevedo, A. C. (2006) *American journal of medical genetics* **140**(23), 2536-2546
8. MacDougall, M., Simmons, D., Luan, X., Gu, T. T., and DuPont, B. R. (1997) *Cytogenetics and cell genetics* **79**(1-2), 121-122
9. Thotakura, S. R., Mah, T., Srinivasan, R., Takagi, Y., Veis, A., and George, A. (2000) *J. Dent. Res.* **79**(3), 835-839
10. Sreenath, T., Thyagarajan, T., Hall, B., Longenecker, G., D'Souza, R., Hong, S., Wright, J. T., MacDougall, M., Sauk, J., and Kulkarni, A. B. (2003) *The Journal of biological chemistry* **278**(27), 24874-24880
11. Suzuki, S., Sreenath, T., Haruyama, N., Honeycutt, C., Terse, A., Cho, A., Kohler, T., Muller, R., Goldberg, M., and Kulkarni, A. B. (2009) *Matrix Biol* **28**(4), 221-229
12. D'Souza, R. N., Cavender, A., Sunavala, G., Alvarez, J., Ohshima, T., Kulkarni, A. B., and MacDougall, M. (1997) *J. Bone Miner. Res.* **12**(12), 2040-2049
13. Sabsay, B., Stetler-Stevenson, W. G., Lechner, J. H., and Veis, A. (1991) *The Biochemical J.* **276** ( Pt 3), 699-707
14. Linde, A., Bhowm, M., and Butler, W. T. (1981) *Biochimica et biophysica acta* **667**(2), 341-350
15. Stetler-Stevenson, W. G., and Veis, A. (1983) *Biochemistry* **22**(18), 4326-4335
16. Veis, A. (1988) *Ciba Foundation symposium* **136**, 161-177
17. George, A., Bannon, L., Sabsay, B., Dillon, J. W., Malone, J., Veis, A., Jenkins, N. A., Gilbert, D. J., and Copeland, N. G. (1996) *J. Biol. Chem.* **271**(51), 32869-32873
18. Sfeir, C., and Veis, A. (1995) *J. Bone Miner. Res.* **10**(4), 607-615

19. Veis, A., Wei, K., Sfeir, C., George, A., and Malone, J. (1998) *European journal of oral sciences* **106 Suppl 1**, 234-238
20. Hao, J., Zou, Bingshuang., Narayanan, K., and George, A. (2004) *Bone* **34**, 921-932
21. He, G., Ramachandran, A., Dahl, T., George, S., Schultz, D., Cookson, D., Veis, A., and George, A. (2005) *J. Biol.Chem.* **280**(39), 33109-33114
22. Alvares, K., Kanwar, Y. S., and Veis, A. (2006) *Dev. Dyn.* **235**(11), 2980-2990
23. Jadlowiec, J., Koch, H., Zhang, X., Campbell, P. G., Seyedain, M., and Sfeir, C. (2004) *J.Biol.Chem.* **279**(51), 53323-53330
24. Malik, R. K., and Parsons, J. T. (1996) *J.Biol.Chem.* **271**(47), 29785-29791
25. Tilghman, R. W., Slack-Davis, J. K., Sergina, N., Martin, K. H., Iwanicki, M., Hershey, E. D., Beggs, H. E., Reichardt, L. F., and Parsons, J. T. (2005) *Journal of cell science* **118**(Pt 12), 2613-2623
26. Golubovskaya, V., Kaur, A., and Cance, W. (2004) *Biochimica et biophysica acta* **1678**(2-3), 111-125
27. Cance, W. G., and Golubovskaya, V. M. (2008) *Science signaling* **1**(20), pe22
28. Mamali, I., Kotsantis, P., Lampropoulou, M., and Marmaras, V. J. (2008) *Journal of cellular physiology* **216**(1), 198-206
29. Howe, A. K., Aplin, A. E., and Juliano, R. L. (2002) *Current opinion in genetics & development* **12**(1), 30-35
30. Aplin, A. E., Stewart, S. A., Assoian, R. K., and Juliano, R. L. (2001) *The Journal of cell biology* **153**(2), 273-282
31. Geiger, B., Spatz, J. P., and Bershadsky, A. D. (2009) *Nature reviews* **10**(1), 21-33
32. Engler, A. J., Sen, S., Sweeney, H. L., and Discher, D. E. (2006) *Cell* **126**(4), 677-689
33. Gilbert, P. M., Havenstrite, K. L., Magnusson, K. E., Sacco, A., Leonardi, N. A., Kraft, P., Nguyen, N. K., Thrun, S., Lutolf, M. P., and Blau, H. M. *Science (New York, N.Y)* **329**(5995), 1078-1081
34. Hynes, R. O. (2004) *Matrix Biol* **23**(6), 333-340
35. Giancotti, F. G., and Ruoslahti, E. (1999) *Science (New York, N.Y)* **285**(5430), 1028-1032
36. Ruoslahti, E. (1988) *Ann. Rev. Biochem.* **57**, 375-413
37. Ruoslahti, E. (1996) *Tumor Biol.* **17**(2), 117-124
38. Staquet, M. J., Couble, M. L., Romeas, A., Connolly, M., Magloire, H., Hynes, R. O., Clezardin, P., Bleicher, F., and Farges, J. C. (2006) *Cell and Tiss.Res.* **323**(3), 457-463
39. Mamali, I., Kapodistria, K., Lampropoulou, M., and Marmaras, V. J. (2008) *J. Cell. Biochem.* **103**(6), 1895-1911
40. Kornberg, L., Earp, H. S., Parsons, J. T., Schaller, M., and Juliano, R. L. (1992) *J.Biol. Chem.* **267**(33), 23439-23442
41. Lim, S. T., Chen, X. L., Lim, Y., Hanson, D. A., Vo, T. T., Howerton, K., Larocque, N., Fisher, S. J., Schlaepfer, D. D., and Ilic, D. (2008) *Molecular cell* **29**(1), 9-22
42. Turner, C. E. (1991) *J.Cell Biol.* **115**(1), 201-207
43. Brown, M. C., West, K. A., and Turner, C. E. (2002) *Molecular biology of the cell* **13**(5), 1550-1565
44. Turner, C. E. (2000) *Nat.cell biol.* **2**(12), E231-236
45. Shemesh, T., Bershadsky, A. D., and Kozlov, M. M. (2005) *J Phys Condens Matter* **17**(47), S3913-3928
46. Jaalouk, D. E., and Lammerding, J. (2009) *Nat. Rev.* **10**(1), 63-73
47. Juliano, R. L., Aplin, A. E., Howe, A. K., Short, S., Lee, J. W., and Alahari, S. (2001)

- Methods in enzymology* **333**, 151-163
48. Aplin, A. E., Hogan, B. P., Tomeu, J., and Juliano, R. L. (2002) *J. Cell Sci.* **115**(Pt 13), 2781-2790
49. Aplin, A. E. (2003) *FEBS letters* **534**(1-3), 11-14

## **Figure Legends**

### **Fig 1**

#### **DPP on the substrate increases C3H10T1/2 cell spreading and adhesion**

C3H10T1/2 cells were seeded on DPP or non-DPP coated coverglass for 30 minutes to 24 hr time points. The cells were fixed and stained for actin. Cells seeded on fibronectin served as positive control.

### **Fig 2**

#### **RGD domain in DPP facilitates cell attachment**

Gold substrate was stamped with DPP on one side and a RGD peptide on the other side. C3H10T1/2 cells were seeded on the substrate for 4 hours, fixed and stained with actin (A1). The stamping pattern is schematically represented (A2). C3H10T1/2 cells were incubated with 1mM or 2mM concentrations of RGD blocking peptide for 2 hours. Cells were then allowed to attach on a DPP coated cover glass and were manually counted with a haemocytometer. Bar graph represents the number of attached cells (B). Scale bar represents 50 $\mu$ m.

### **Fig 3**

#### **Identification of the cell surface alpha and beta integrin specific for DPP ligand**

Receptor-cell binding experiments were performed by incubating C3H10T1/2 cells with either  $\alpha$ v,  $\alpha$ 4,  $\alpha$ 5,  $\beta$ 5,  $\beta$ 4,  $\beta$ 3 and  $\beta$ 1 antibodies for 2 hours respectively. The combination of cells with the integrin antibodies were seeded on DPP coated plates and incubated for 24 hrs. Light microscopic images (Zeiss, NY) of the cells on DPP coated plates were imaged (A). Note the

specificity of the  $\alpha v$  and  $\beta 1$  antibodies. Specificity was confirmed by isolating membrane proteins and western blots were performed using  $\alpha v$  and  $\beta 1$  integrin antibodies (B). SiRNA transfection of  $\beta 1$  integrin was performed in C3H10T1/2 cells grown on DPP coated plate. 0.5 $\mu$ g of the siRNA was used for transfection. Transfection performed with scramble siRNA was used as the control (C).

#### **Fig 4**

##### **DPP triggers the organization of Focal Adhesion Complexes**

C3H10T1/2 cells were seeded on DPP coated plates for 16 (A1) and 24hr (A2). Immunohistochemical analysis was performed with paxillin (red) and FAK (green) antibodies. Confocal microscopic images are presented in (A). Immunostaining indicate the successful spreading and formation of focal adhesions. FAK is localized at focal adhesions and the nucleus (single arrow), while paxillin is localized predominantly at focal adhesions. “Z” stack analysis was performed to determine colocalization of FAK with paxillin at 24 hour time point (B). DPP induces *in vivo* association of FAK and paxillin (C). 50  $\mu$ g total protein and FAK antibody was mixed with protein A-beads and incubated overnight is represented as "T". The beads were then washed with PBS, SDS-PAGE loading dye was added to the beads and boiled. Immunoblot was performed with paxillin antibody. "C" represents immunoprecipitation performed in the absence of FAK antibody. C3H10T1/2 cells were seeded on DPP coated plates and total proteins were isolated at various time points as indicated and western blot was performed to determine activation of FAK (D) and paxillin (E). Total proteins isolated from C3H10T1/2 cells grown in the absence of DPP were used as control "c".

#### **Fig 5**

##### **Cells on DPP substrate promotes actin polymerization**

C3H10T1/2 cells were transfected with an mRFPruby-actin plasmid using Fugene HD. The cells were then trypsinized and were seeded on a DPP coated cover glass. Confocal microscopic images were taken at 8 (A1) and 24 hours (A2). Note incorporation of the mRFPruby-actin into subcompartments of the actin cytoskeleton such as lamellipodium (single arrow), filapodia

(single arrowheads) and stress fibers (double arrowheads).

## **Fig 6**

### **Activation of ERK1/2 MAPK pathway by adherent cells on DPP substrate**

C3H10T1/2 cells were seeded on DPP coated plates and were treated with or without PD98059 for 4 and 24hrs. Total proteins were isolated and western blots were performed using pERK1/2 and tubulin antibodies. Cells in suspension were used as control (A). Confocal imaging was performed on adherent cells at 24hrs. No nuclear localization was observed in cells seeded on tissue culture cover glass (B1) Nuclear localization of pERK1/2 was seen in cells plated on DPP coated coverglass (B2) and this was inhibited after PD98059 treatment for 24 hrs (B3).

## **Fig 7**

### **Cells adherent on DPP stimulates nuclear accumulation of ELK-1 transcription factor**

Confocal image of ELK-1 immunostaining performed on C3H10T1/2 cells seeded on DPP coated coverglass (A). A transient transfection of FLAG construct of ELK-1 was performed using Superfect reagent on C3H10T1/2 cells seeded on DPP coated plates. Localization of ELK-1 was determined by immunofluorescence with an ELK-1 antibody and TRITC-conjugated anti-rabbit secondary antibody. Nuclear localization of ELK-1 was in the DPP treated plates (B). Cells seeded on tissue culture plate were used as control(C). Scale bar is 20 $\mu$ m.

## **Fig 8**

### **Blocking RGD abrogates the activation of FAK, Paxillin and ERK1/2**

C3H10T1/2 cells were incubated with 2mM RGD peptide at room temperature for 2 hrs. The cells were then seeded on DPP coated plates. Total protein was isolated after 24 hrs and immunoblotting was performed with anti- phospho ERK1/2, phospho FAK, phospho paxillin and tubulin antibodies. Cells seeded on DPP coated plate was used as control.

## **Fig 9**

### **DPP induces odontogenic differentiation in C3H10T1/2 cells**

C3H10T1/2 cells were seeded on DPP coated plates for 4 and 24 hrs. Total RNA was isolated and subjected to real time PCR and analyzed for the expression of Runx2, DSP, DMP1, BMP4, BSP, OPN, MMP9 and osteocalcin. GAPDH was used as the house keeping gene.

## **Fig 10**

### **DPP triggers nuclear localization and protein synthesis of odontogenic markers of differentiation**

Total protein was isolated from cells seeded on DPP coated plates at 4, 24 and 48h and immunoblotting was performed with DMP1, DSP, DPP and tubulin antibodies (A). Cells seeded on tissue culture plate for 48 hrs were used as control.

Confocal image of C3H10T1/2 cells seeded on DPP coated coverglass for 24 hrs and immunostained using antibodies for DSP, DMP1 and RUNX2 (B). Nuclear localization of DSP, DMP1 and RUNX2 were seen in cells plated on DPP coated coverglass.

## **Fig 11**

### **DPP plays an important role in the terminal differentiation of odontoblast.**

C3H10T1/2 cells seeded on DPP coated plates were grown in mineralization media for 7, 14 and 21 days. Light microscopic picture of the cells in the presence and absence of mineralization media at 21 day were taken (A). Change in the morphology of the cells were observed in the absence (Aa) and presence (Ab) of mineralization media. RNA was extracted using TRIzol at 7, 14 and 21 days and real time PCR was performed for RUNX2, DSP and DMP1 (B). Total proteins were isolated from C3H10T1/2 cells seeded on DPP coated plates grown under mineralization condition for 7, 14 and 21 days (C). Immunoblot was performed with DSP, DMP1, DPP and pERK1/2. Total proteins isolated from cells grown on DPP coated plates for 21

days in the absence of mineralization media was used as control.

### **Fig 12**

#### **DPP triggers mineralized nodule formation in C3H10T1/2 cells**

von kossa staining was performed on C3H10T1/2 cells seeded on DPP coated plates grown in mineralization media for 7, 14 and 21 days (A). The cells were fixed in formalin, washed twice with distilled water and then stained with 1% silver nitrate solution. von Kossa staining demonstrated a high intensity of dark staining pattern at 14 and 21 days of culture. Cells grown on DPP coated plates without mineralization media (B) and cells on tissue culture plate with mineralization media(C) were used as a controls.

### **Fig 13**

#### **DPP induces matrix mineralization in C3H10T1/2 cells.**

C3H10T1/2 cells seeded on DPP coated plates were grown in the presence of mineralization for 7, 14 and 21 days (A). Matrix mineralization is indicated by the red areas as a result of calcium staining with Alizarin Red. As controls, cells were grown in mineralization conditions on tissue culture plates for 7, 14 and 21 days (B).

### **Fig 14**

#### **Hypothetical model**

Hypothetical model depicting the RGD mediated integrin anchorage of cells on DPP and the subsequent activation of focal adhesion complexes and downstream gene transcription.

#### **Acknowledgement:**

This work was supported by National Institutes of Health Grant DE 19633 and the Brodie

Endowment Fund. We are grateful to Drs Sriram Ravindran, Tanvi Muni and Qi Gao for providing assistance with the confocal imaging and cell culture.

Fig:1

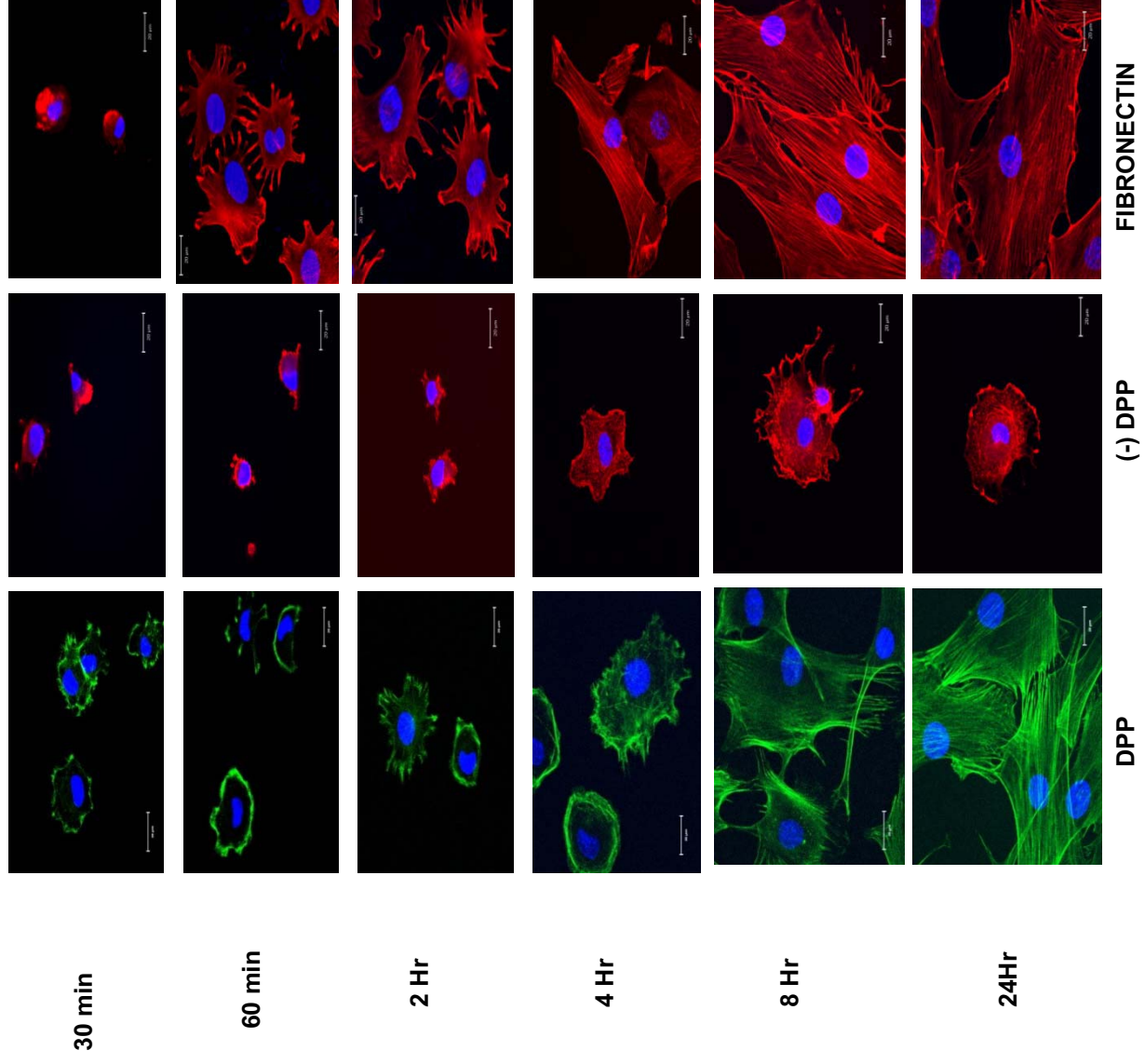
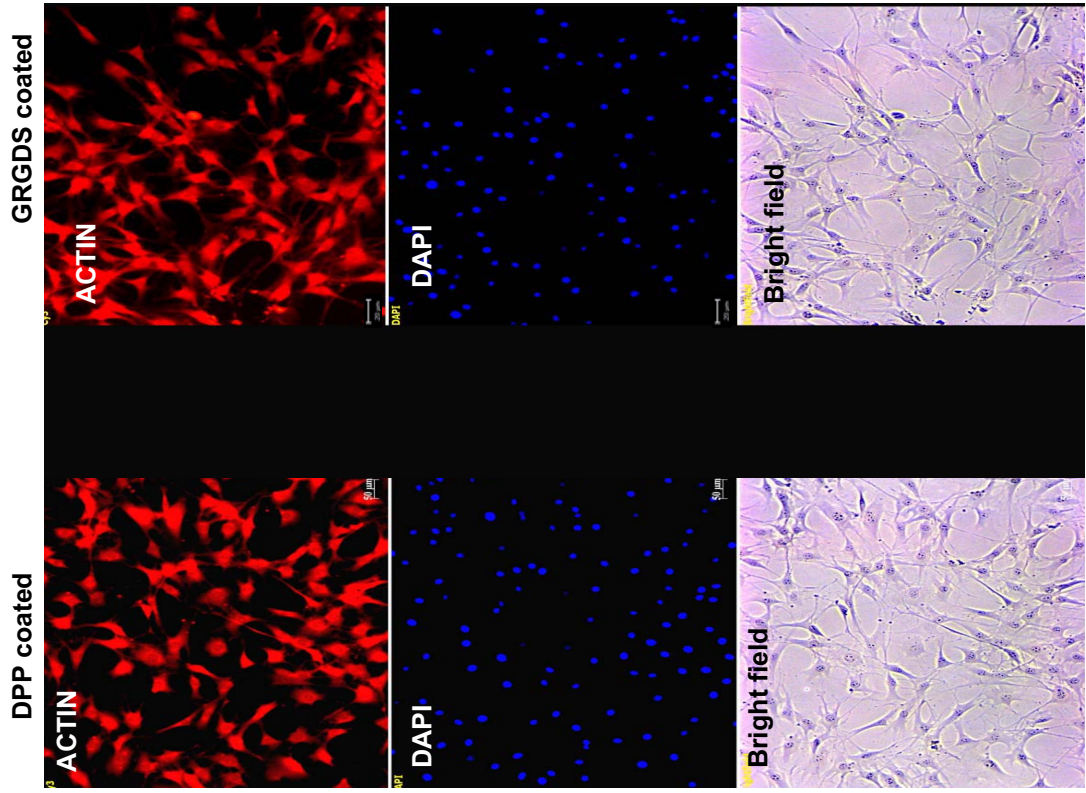
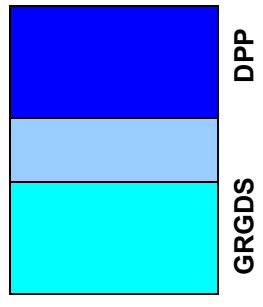


Fig:2

A1



A2



B

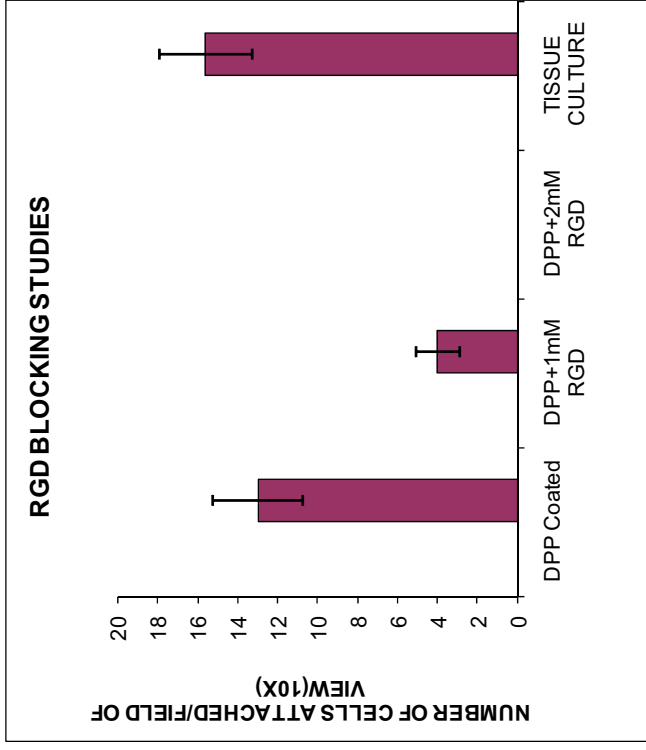
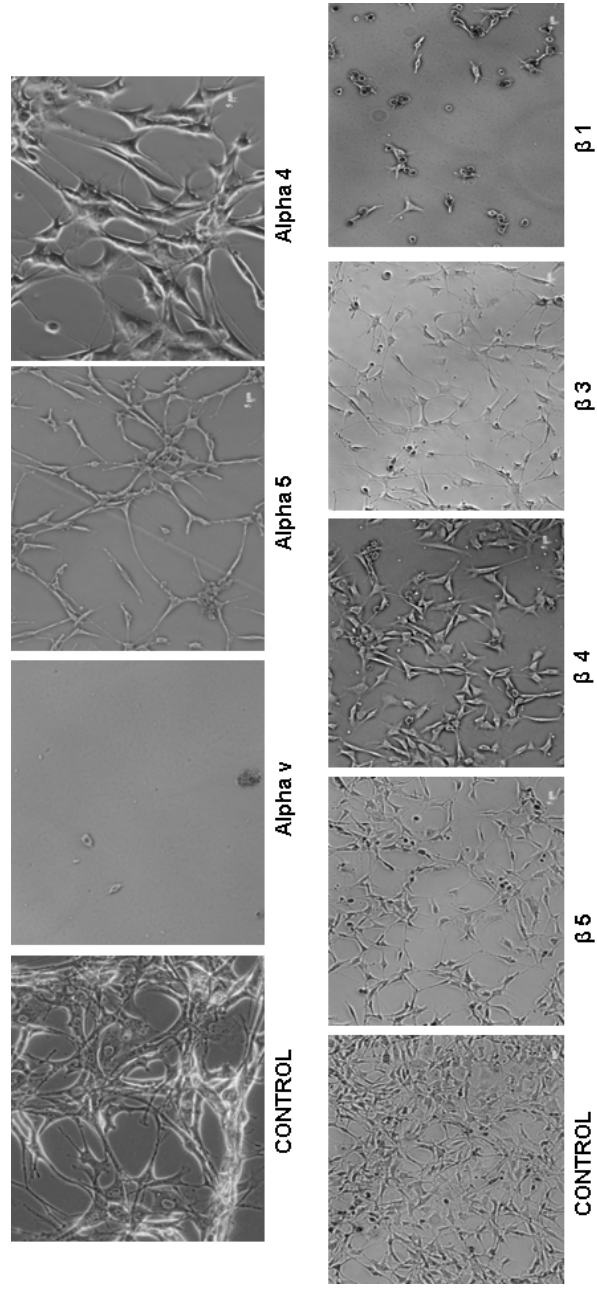
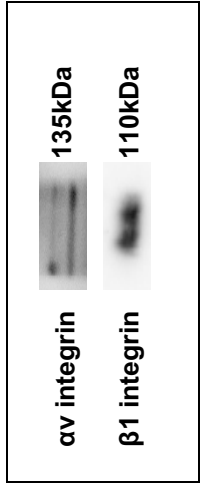


Fig:3

**A**



**B**



**C**

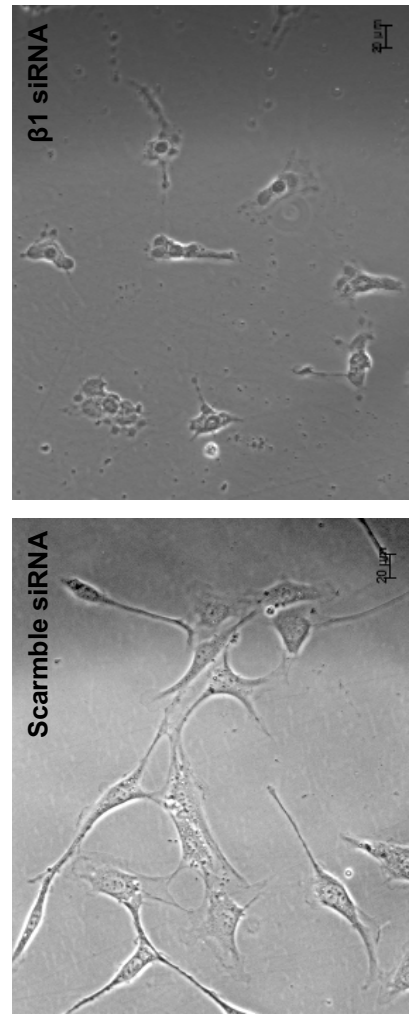
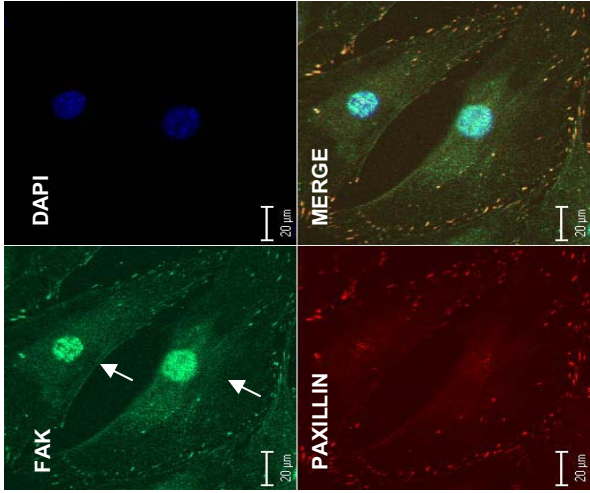
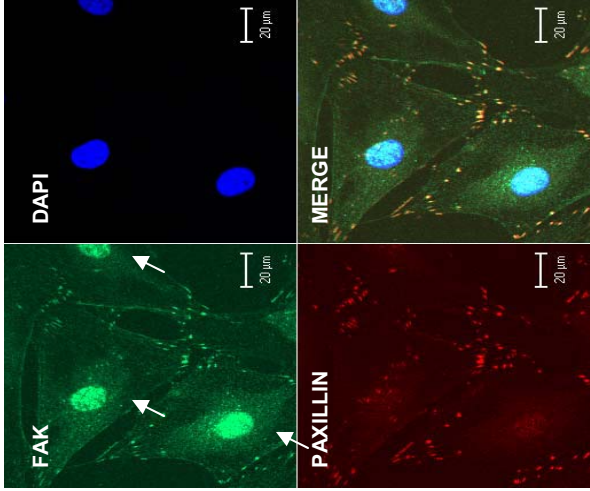


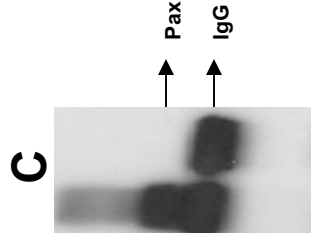
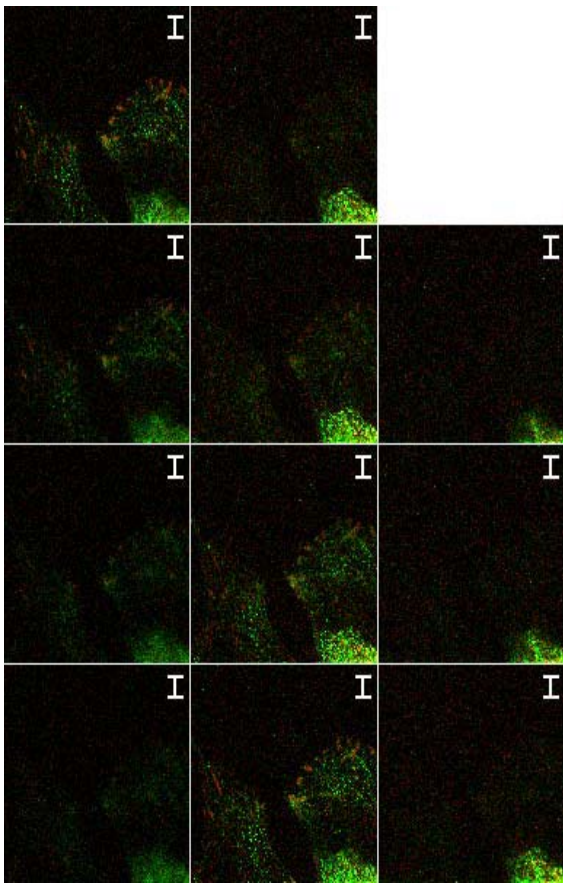
Fig:4 A1



A2

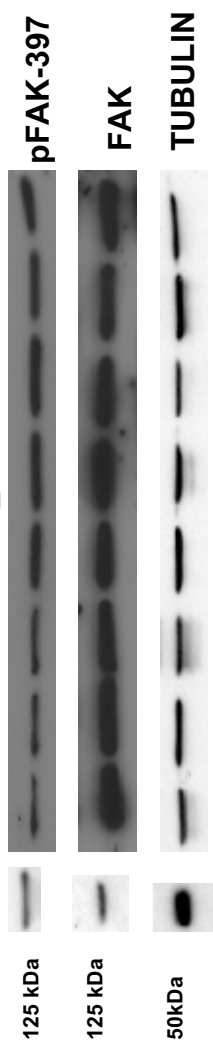


B



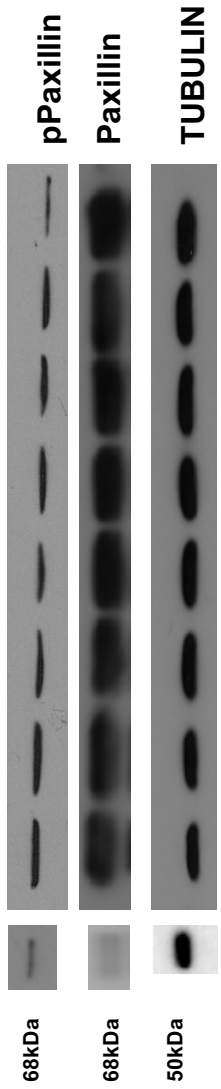
IP: FAK  
WB: PAXILLIN

D



C 30' 60' 2h 4h 8h 16h 20h 24h

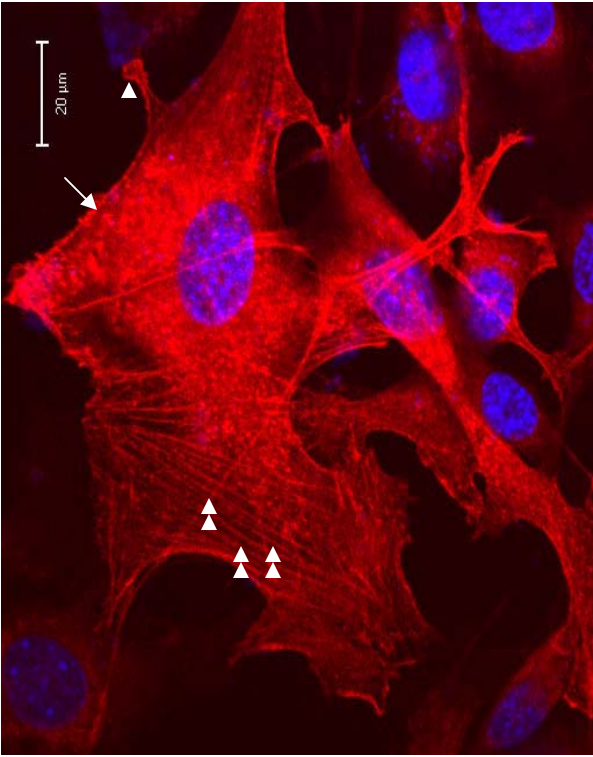
E



C 30' 60' 2h 4h 8h 16h 20h 24h

Fig:5

A1



A2

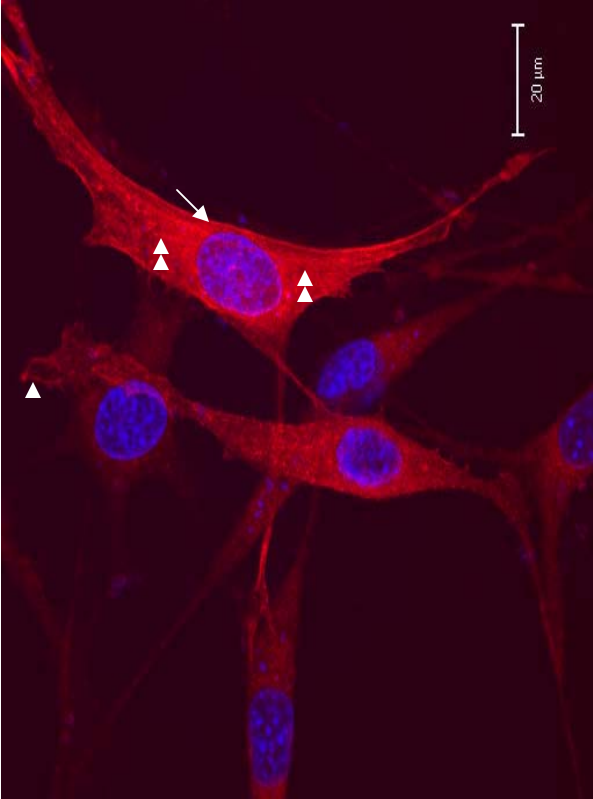


Fig: 6

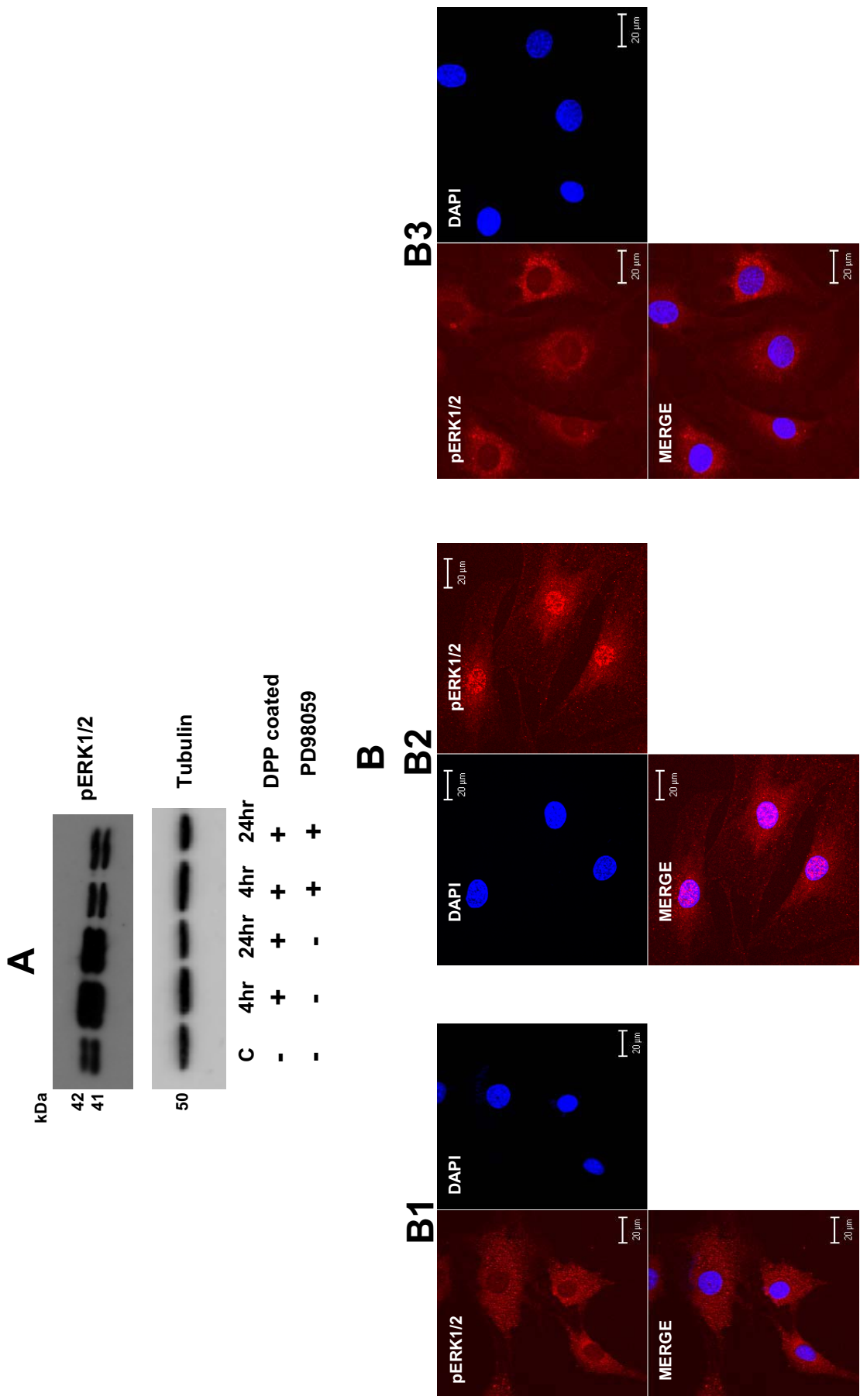
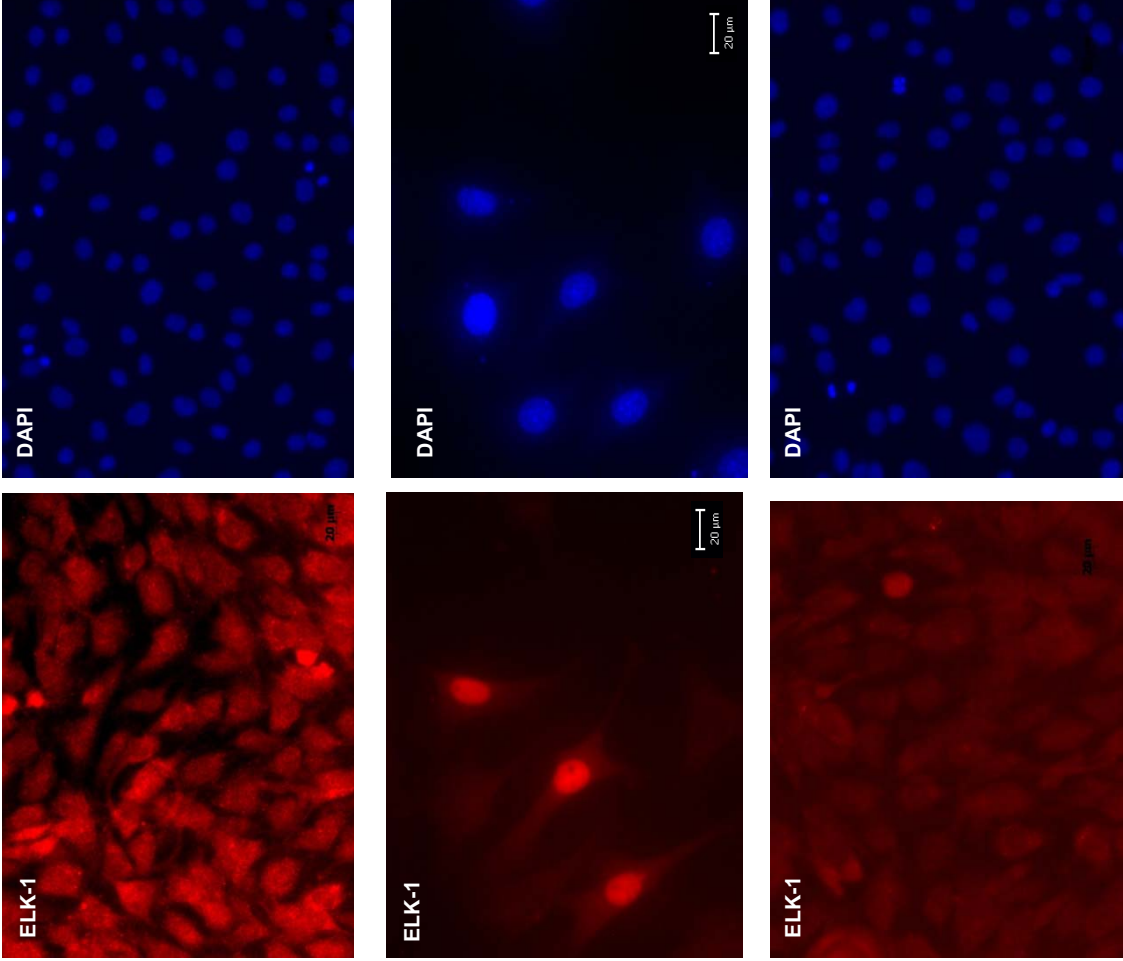


Fig:7



**A**

**B**

**C**

Fig:8

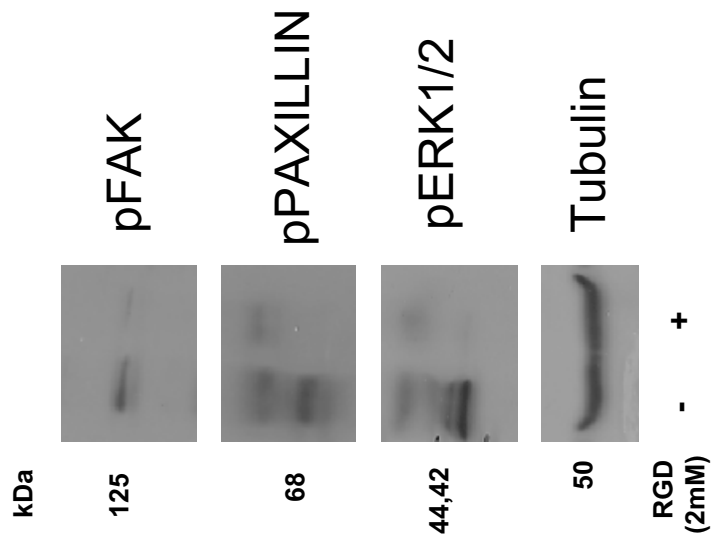


Fig:9

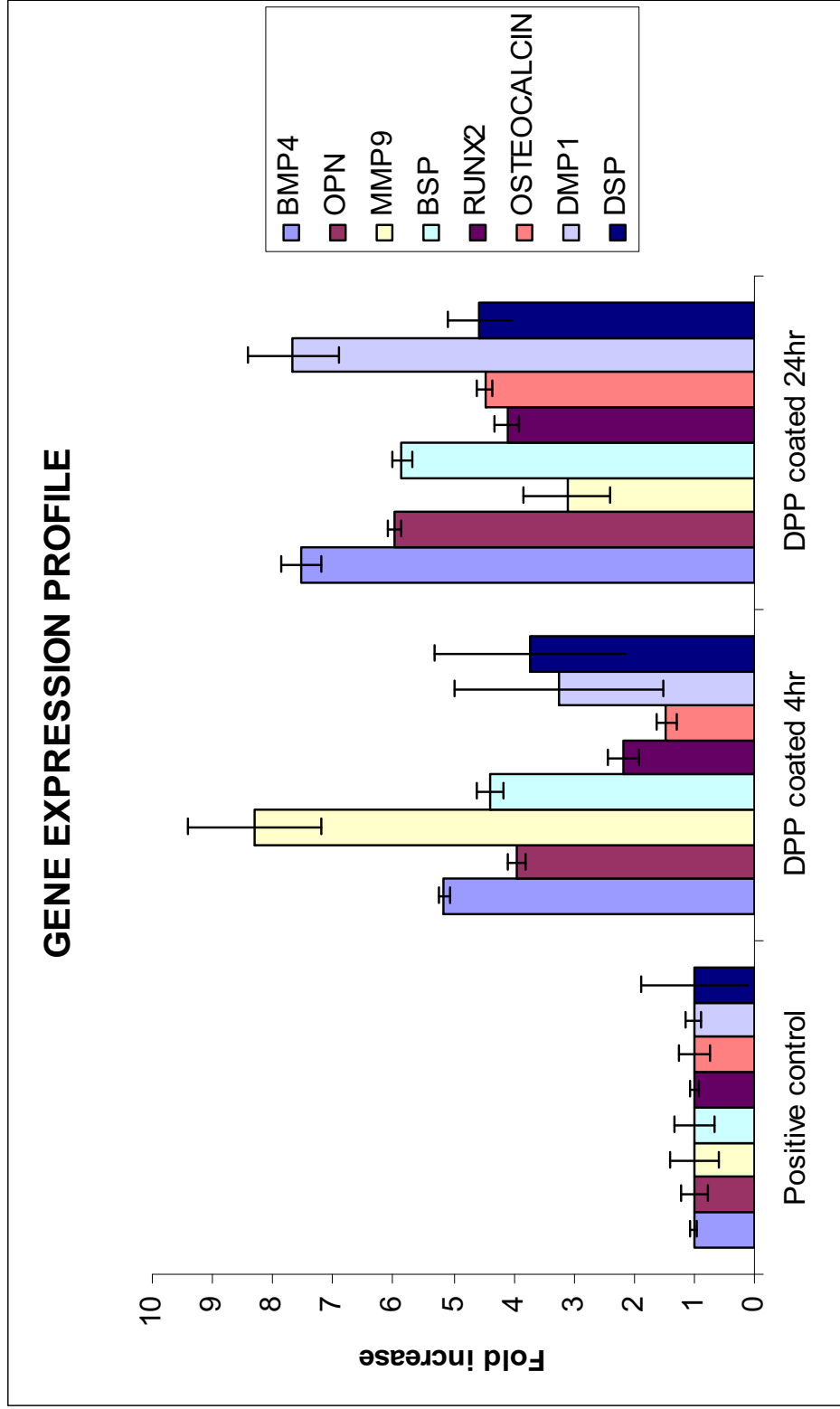


Fig:10

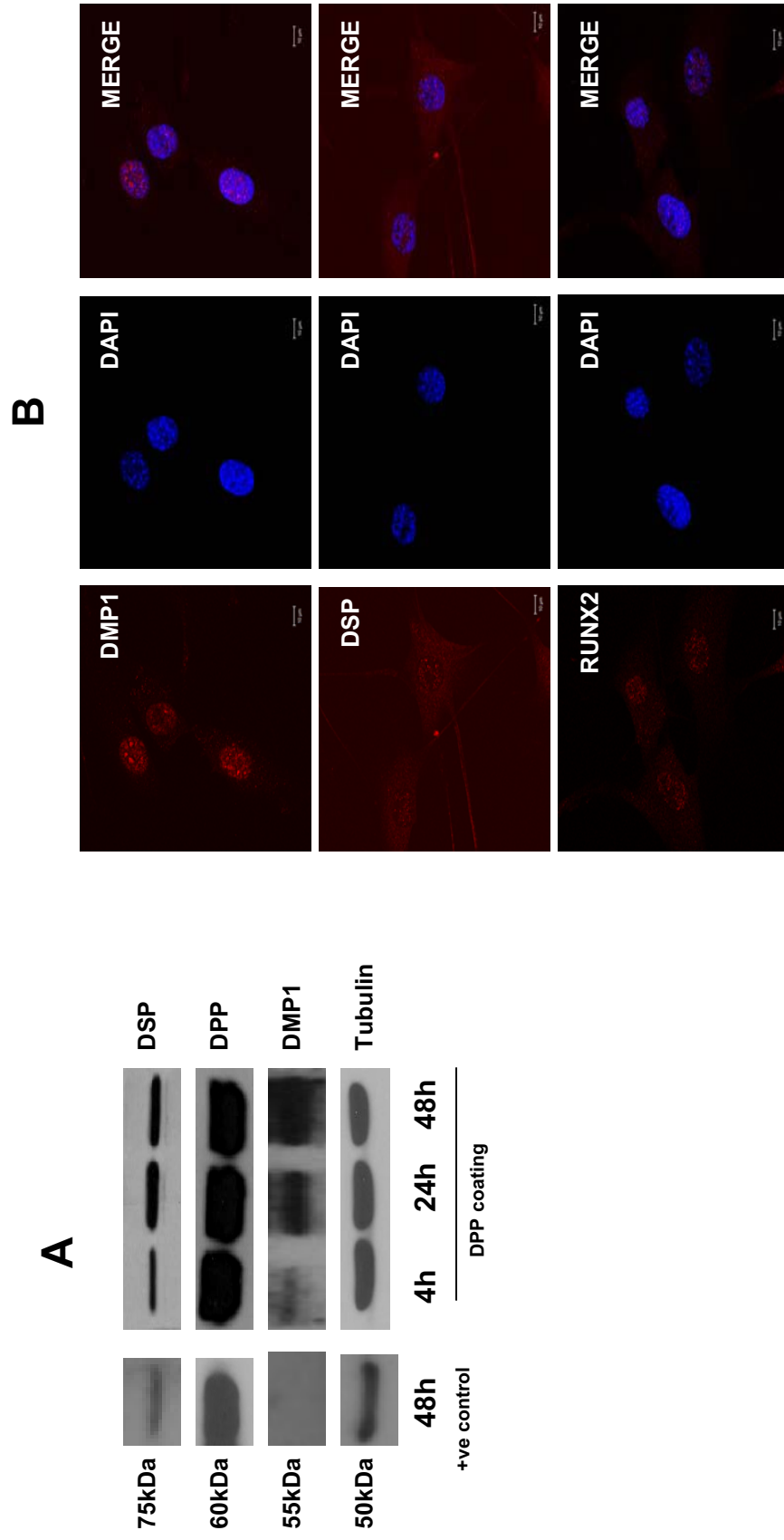
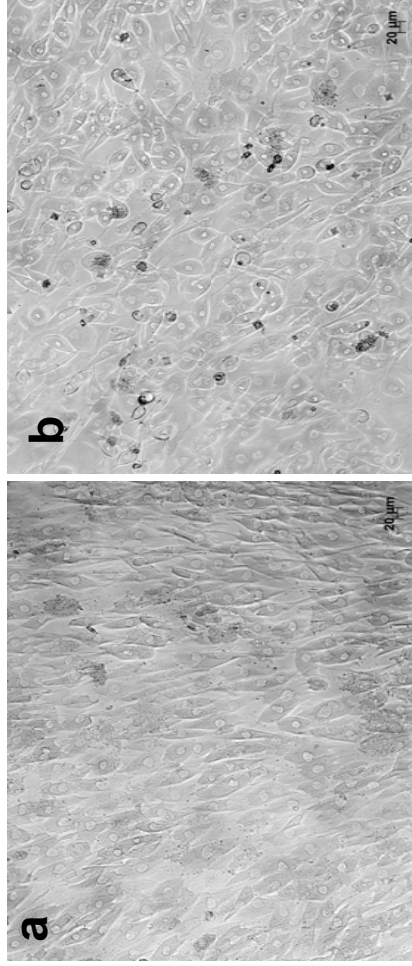
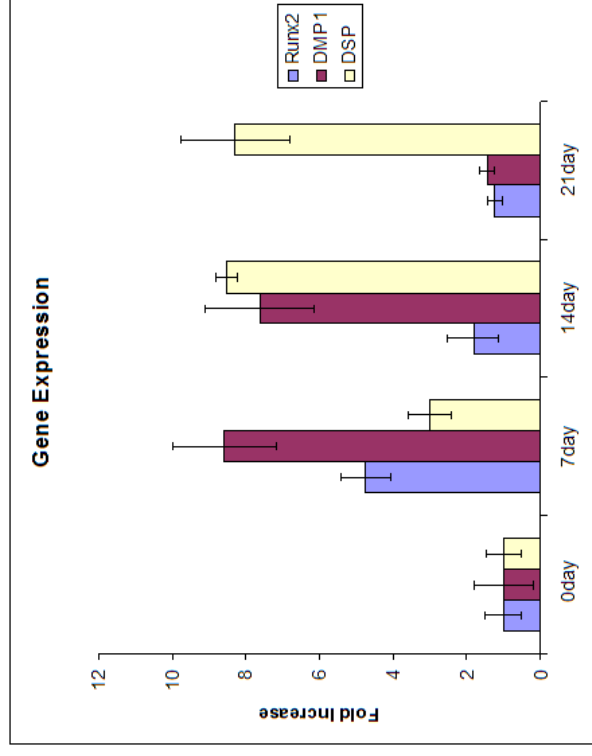


Fig:11

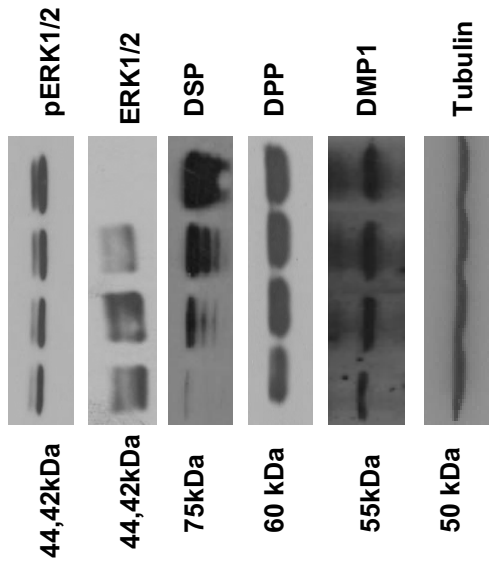
**A**



**B**



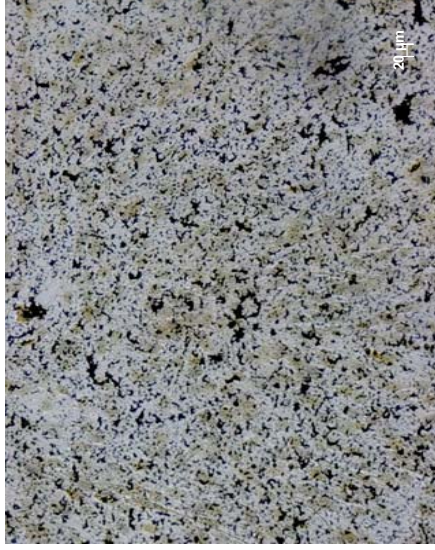
**C**



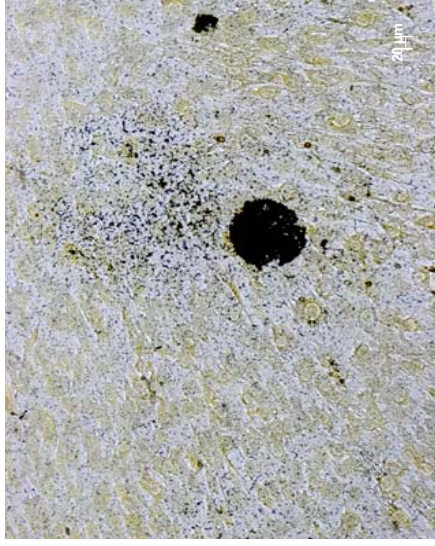
0 7D 14D 21D

DPP coating and mineralization

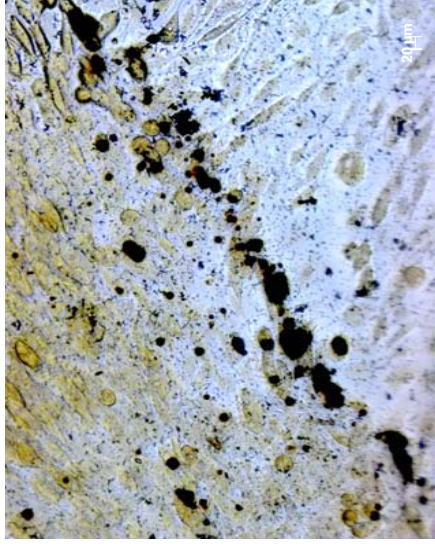
Fig:12



7 DAY

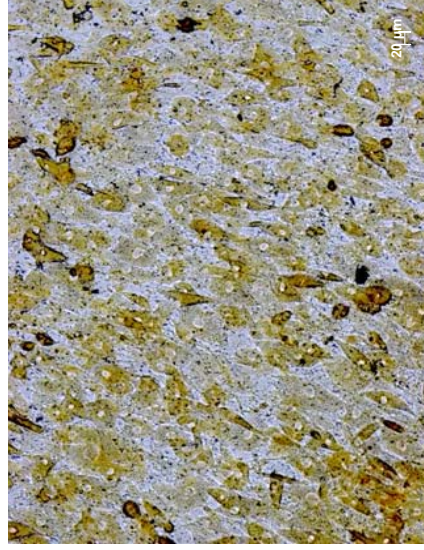


14 DAY



21 DAY

**B**



**C**

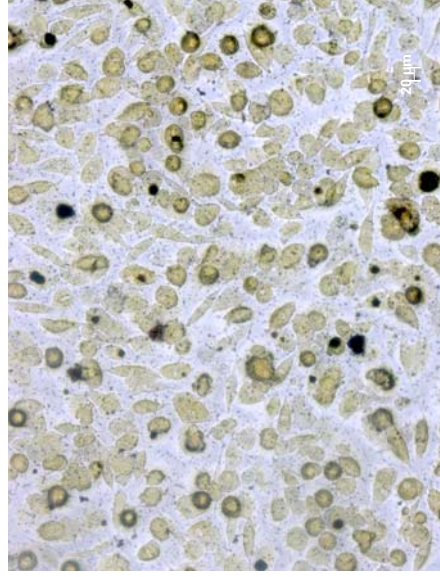
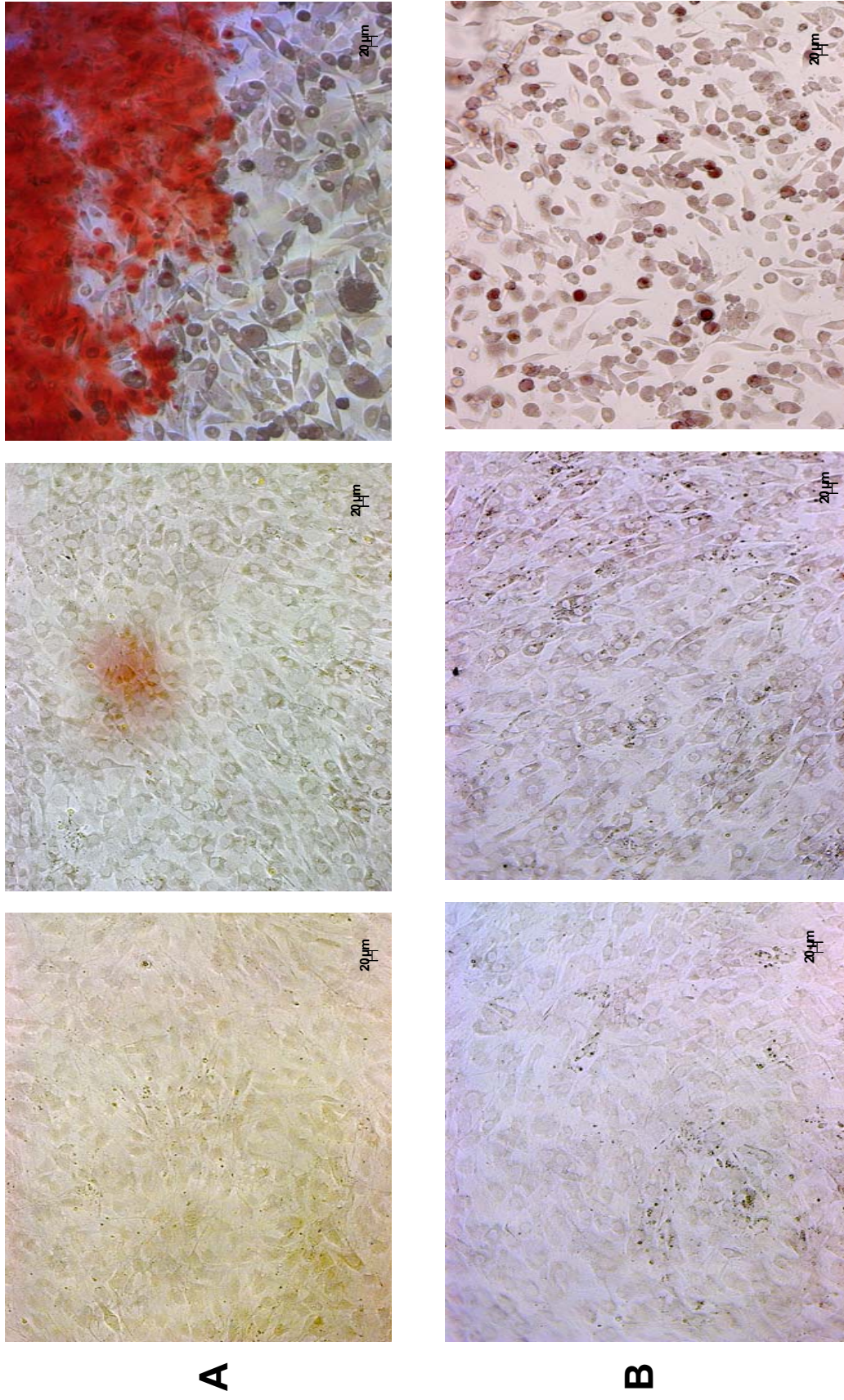


Fig:13



**A**

**B**

7 Day

14 Day

21 Day

FIG: 14

